AD-A188 026 THE PIERCE DIODE WITH AN EXTERNAL CIRCUIT I SIMULATIONS 1/1
IN THE LINEAR REG (U) CALIFORNIA UNIV BERKELEY
ELECTRONICS RESEARCH LAB W S LAWSON 22 JUL 87
UNCLASSIFIED UCB/ERL-M87/51 N00014-85-K-0809 F/G 9/1 NL

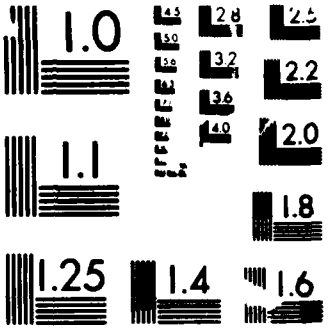

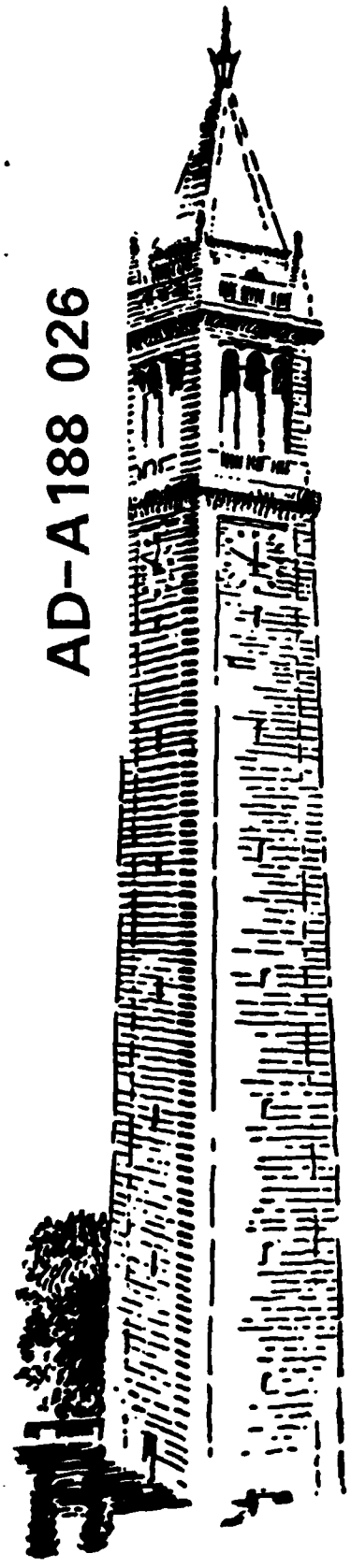

THE PIERCE DIODE WITH AN EXTERNAL CIRCUIT. I. SIMULATIONS IN THE LINEAR REGIME

by

William S. Lawson

Contract N00014-85-K-0809

Memorandum No. UCB/ERL M87/51

22 July 1987

ELECTRONICS RESEARCH LABORATORY

College of Engineering

University of California, Berkeley, CA 94720

THE PIERCE DIODE WITH AN EXTERNAL CIRCUIT. I. SIMULATIONS IN THE LINEAR REGIME

by

William S. Lawson

Memorandum No. UCB/ERL M87/51

22 July 1987

ELECTRONICS RESEARCH LABORATORY

College of Engineering
University of California, Berkeley
94720

THE PIERCE DIODE WITH AN EXTERNAL CIRCUIT. I. SIMULATIONS IN THE LINEAR REGIME

William S. Lawson

15 July 1987

Abstract

The linear theory for the eigenfrequencies of the extended Pierce diode for resistive, capacitive, and inductive external circuits is tested via computer simulation with the PDW1 code, and is verified to within the accuracy of the simulation (between 1% and .01% depending on the circumstances). The simulations were remarkably inexpensive in terms of computer time, and could have been performed on a personal computer.

Introduction

The classical Pierce diode is a theoretical model with relevance to several bounded plasma devices. It consists of two electrodes (either plates or grids) a distance l apart, connected by a short circuit, with a beam of electrons injected at one electrode with constant velocity v_0 and absorbed at which ever electrode is first encountered. The electron beam is neutralized by infinitely massive co-moving ions (see Fig. 1). Pierce showed [1] that the behavior of this device is governed solely by the dimensionless parameter $\alpha = \omega_p l/v_0$ where ω_p is the plasma frequency of the incoming beam of electrons. (Pierce assumed stationary ions, which made no difference in his model, but for the extended model presented here, the distinction is important.) Pierce also worked out the dispersion relation for linear perturbations about the uniform equilibrium. This dispersion relation is

$$\frac{2\theta\alpha^2}{(\theta^2+\alpha^2)^2}\left(1-e^{-\theta}\cos\alpha\right)+\frac{\alpha(\alpha^2-\theta^2)}{(\theta^2+\alpha^2)^2}e^{-\theta}\sin\alpha+\frac{\theta^2}{\theta^2+\alpha^2}=0 \qquad (1)$$

where θ is the normalized complex temporal growth rate, *i.e.*, $\theta = \frac{l}{v_0}(\gamma + i\omega)$. Despite appearances, there is no singularity at $\theta = \pm i\alpha$. The standard Pierce model has been studied by several people. Pierce found the value of α which first becomes unstable, Cary and Lemons [2] correctly described the dominant branch of the dispersion curve, and Crystal and Kuhn [3] have successfully verified the linear behavior of the classical Pierce diode using the computer particle simulation code PDW1 [4]. Crystal and Kuhn also investigated some of the non-linear saturation states via the same simulation methods.

In an effort to understand the effects of an external circuit on bounded plasma systems, Kuhn [5] replaced the external short circuit with a series RL circuit, and found the linear modes of the plasma/circuit system (which I shall refer to as the extended Pierce diode). Kuhn and Hörhager [6] generalized this to a series RLC circuit, worked out the dispersion relation, and graphed the eigenvalues for the R, L, and C elements taken separately. The modified dispersion relation is

$$\frac{2\theta\alpha^2}{(\theta^2+\alpha^2)^2}\left(1-e^{-\theta}\cos\alpha\right)+\frac{\alpha(\alpha^2-\theta^2)}{(\theta^2+\alpha^2)^2}e^{-\theta}\sin\alpha+\frac{\theta^2}{\theta^2+\alpha^2}+C^{-1}+R\theta+L\theta^2=0 \qquad (2)$$

(Kuhn and Hörhager multiply (1) by $(\theta^2+\alpha^2)^2$ to clear the denominator, but this introduces spurious double roots at $\theta=\pm i\alpha$.)

It is my purpose to use computer simulation (the PDW1 code) to verify the linear theory of Kuhn and Hörhager for specific values of α.

Choice of Parameters

Because the regime of interest is linear, and particles' deviations from their unperturbed positions is small, great accuracy can be achieved with minimal numbers of particles and grid points. Most of the simulation runs were performed with 128 particles (on the average) and 128 grid cells, with the time step chosen such that each particle moves roughly one grid cell per time step. With these modest parameters, it is possible to follow the decay of a mode through twenty or more decades in amplitude. The complete simulation parameters are shown in Table I. These simulation parameters make the θ representation (Equation 2) most appropriate (see Kuhn and Hörhager for a description of the alternate η representation).

The simulation eigenvalues (values of θ) were obtained from the simulation as a function of time, using a four-time-point scheme due to Buneman [7] when the expected dominant mode has a single complex frequency, and by a two-time-point scheme when it has a purely growing or purely damped frequency. (The scheme of Buneman can be extended to yield the two most dominant modes if both are purely growing or damped; this extension was used in some cases in which the modes were so close together in θ that the sub-dominant mode did not decay enough for an accurate measurement of the damping rate of the dominant mode.) The eigenvalues obtained by this scheme will be exact only when there are no competing modes. When competing modes are present, the error in the computed values of the eigenvalues will be proportional to the amplitude of the competing mode.

In order to estimate the precision of the simulation results, the eigenvalues given by the simulation (estimates of θ) are plotted as a function of time and as a table of numbers. Typically, these plots begin by fluctuating strongly, then settle down to a fairly constant value, then begin to fluctuate again, either due to non-linearity (when the mode is growing), or round-off noise (when the mode is damped). Figure 2 shows an example of this behavior for the classical Pierce diode at $\alpha = \pi/2$ (the first entry in Table II). The minimum fluctuation about this constant value is given in the tables of results as an estimate of the precision of the simulation.

The errors listed in the tables are *not* meant to reflect the *accuracy* of the simulations, but rather the *precision* with which the simulation produces its result. The actual error also includes systematic errors which can be only roughly estimated knowing the order of accuracy of the algorithms. The particle integrator is accurate to second order in all cases, but the circuit advancement algorithm is of different orders for different external circuit elements. These circuit advancement algorithms will be discussed as the results for the respective circuits are discussed.

The α values $\pi/2$, $3\pi/2$, and $5\pi/2$ were chosen for simulation. These values of α have nearly maximal separation between the dominant mode and the next most dominant one, thus ensuring that, in most cases, after a reasonable amount of time, only the dominant mode will be significant. These values for α have the additional advantage that they sample each of the three different types of behavior of the classical Pierce diode, namely dominant modes which are monotonically damped, monotonically growing, and oscillatory growing.

Initially, the beam fills the simulation region uniformly except for a sinusoidal perturbation in position. This perturbation is chosen to give the dominant mode an advantage over the other modes. The density profile for the dominant mode is never truly sinusoidal, but the modes are similar to sinusoids.

The external circuits also require initial conditions. Recall that the average current of the beam (which is quite large) is neutralized by the co-moving ions in order to prevent a large offset voltage in the resistive case, and the build-up of charge in the capacitive case. Thus the external circuit must respond only to the perturbation. The initial conditions for the resistive and inductive circuits present no special problems, since only the initial voltage and current need be specified, and regardless of how they are chosen, the dominant mode will eventually take over. The initial conditions for the capacitive case, however, have an additional complication. The charge on the emitting electrode minus the charge Q on the capacitor is a constant; hence, if the unperturbed

state (uniform beam, zero voltage across the diode) is to be an allowed state of the system, then the initial charge on the capacitor must be chosen to be equal to the initial charge on the emitting electrode. This condition can be satisfied by choosing the initial condition for the charge on the external capacitor consistently with the initial electric field at the emitting electrode (which is proportional to the charge on the electrode according to Gauss' law). This choice is essential, but fortunately requires only a little algebra.

Simultion Results

(a) Capacitive Case

When the external circuit consists of a capacitor, it is to be expected that the smaller the capacitance, the more damped each of the modes is, since the limit $C \to 0$ reduces to the open circuit case which shows no instability. The stabilizing effect of the external capacitor can be seen in Fig. 3 (taken from Kuhn and Hörhager — who denote the normalized circuit quantities with overbars, whereas here the overbars are omitted). Figure 3a shows the real parts of the growth rates as a function of α for several values of $1/C$, and Figure 3b shows the imaginary part of the same growth rates.

The simulation results for the capacitive case (including the $C = \infty$ case, which is the classical short circuit Pierce diode), are shown in Table II. The systematic error is of second order in the time step (roughly 0.01 percent), since the circuit is an instantaneous boundary condition on the solution of Poisson's equation. Confirmation of the linear theory is plain.

(b) Resistive Case

One might expect an external resistance to have the same sort of stabilising effect that a capacitor has, but this is not the case. Figure 4 (also from Kuhn and Hörhager) shows the dispersion plots for several resistance values. An external resistor does not reduce the real parts of *all* growth rates, but rather, for large resistances, tends to reduce their magnitudes, bringing them closer to zero, which implies the existence of a static mode in the limit $R \to \infty$. This seems to be a paradox, since the $R \to \infty$ limit should be an open circuit, just as with the $C \to 0$ limit. The reason for this apparent paradox is the extra initial condition which was imposed on the capacitive case in order to make the unperturbed state accessible. For large values of the resistor, the circuit becomes an RC circuit perturbed by the plasma where the capacitance comes from the parallel plate capacitance of

the confining electrodes. The relaxation time of this RC circuit grows in proportion to R, so the growth rates (or at least the dominant growth rate) must approach zero as $1/R$.

The results for the resistive case are shown in Table III. Again, the confirmation is clear, although the discrepancy between theory and simulation is about one percent. The method used for advancing a resistive circuit in time is, however, only first-order accurate in the time step, so an error of a percent is to be expected.

(c) Inductive case

An external inductor is also a stabilizing influence in most cases. As one might expect, the higher frequency modes are affected the most. Figure 5 (again from Kuhn and Hörhager) shows the dispersion plots for several inductance values.

There is one exception to the stabiizing influence of the external inductor. Surprisingly, it occurs in the most stable regime of the classical Pierce diode — the $\alpha < \pi$ regime. A new mode is observed, which is stable for some values of L, and unstable for others. Figure 6 shows the real and imaginary parts of the growth rate of this mode for $\alpha = \pi/2$ versus the logarithm of L. The imaginary part of the growth rate reveals that this mode is in essence an LC oscillation perturbed by the plasma, where the capacitance comes from the vacuum capacitance of the bounding electrodes. As the value of L decreases, the imaginary part of the growth rate (*i.e.*, the frequency) increases as the inverse square root of L. Expanding the growth rate $Re\,\theta$ for small α and small $Re\,\theta$ yields

$$Re\,\theta \approx \frac{\alpha^2}{2}\sqrt{L}\left(\sin\frac{1}{\sqrt{L}} + 2\sqrt{L}\cos\frac{1}{\sqrt{L}}\right) \tag{3}$$

Since only the magnitude of the growth or decay depends on α, and not whether the mode is stable or not, a transit time effect is indicated rather than a true plasma interaction.

The principal results for the inductive case are shown in Table IV. Once again, the theory is confirmed to high accuracy.

As mentioned above, the LC mode has the interesting property that it can be unstable in the $\alpha < \pi$ regime, which is stable for all other external circuits. Note that Fig. 6 shows the beginning of an infinite progression of stable and unstable regions as $L \to 0$. These modes are somewhat difficult to simulate, since the imaginary part of θ (the frequency) varies as $1/\sqrt{L}$, and so becomes very large for small values of L. The difficulties can be overcome by a very small time step, however, and

Table V shows the results for eight values of L (each at a different extremum of the real part of the growth rate curve shown in Fig. 6). The agreement is surprisingly good.

Summary

The extended Pierce diode of Kuhn and Hörhager has been simulated with great accuracy, confirming their linear theory in all cases.

Acknowledgements

I gratefully acknowledge the help of Dr. T. L. Crystal, Prof. S. Kuhn, and Prof. C. K. Birdsall. This work was supported by the Department of Energy contract DE-AT03-76ET53064 and Office of Naval Research contract N00014-85-K-0809.

References

[1] J. R. Pierce, *J. Appl. Phys.* 15(1944), 721

[2] J. R. Cary and D. S. Lemons, *J. Appl. Phys.* 53(1982), 3303

[3] T. L. Crystal and S. Kuhn, *Phys. Fluids* 28(1985), 2116

[4] Wm. S. Lawson, "PDW1 User's Manual", University of California, Berkeley, Electronics Research Lab memo UCB/ERL M84/37, 1984

[5] S. Kuhn, *Phys. Fluids* 27(1984), 1834

[6] S. Kuhn and Hörhager, *J. Appl. Phys.* 60(1986), 1952

[7] O. Buneman, *J. Comp. Phys.* 29(1978), 295

System length	1
Number of grid cells	128
Time step	1/128
Number of time steps	1024
ϵ_0	1
q_e/m_e	-1
m_i	∞
v_0	1
Injected electron current	$-\alpha^2$
Background current	α^2
Injected electron flux	128

Table I. Simulation parameters

CAPACITIVE CASE

C	Theory	Simulation	α
∞	-1.9269	$-1.9272 \pm .0002$	$\pi/2$
20	-2.0120	$-2.0122 \pm .0002$	
10	-2.0926	$-2.0928 \pm .0002$	
5	-2.2420	$-2.2423 \pm .0003$	
∞	0.76575	$0.76591 \pm .00001$	$3\pi/2$
20	0.57219	$0.57238 \pm .00001$	
10	0.38749	$0.38770 \pm .00001$	
5	0.04056	$0.04088 \pm .00002$	
∞	$0.5892 + 1.4289i$	$0.5898 \pm .0002 + (1.4296 \pm .0002)i$	$5\pi/2$
20	$0.4602 + 1.7399i$	$0.4605 \pm .0001 + (1.7404 \pm .0002)i$	
10	$0.3389 + 1.9831i$	$0.3393 \pm .0002 + (1.9833 \pm .0001)i$	
5	$0.1162 + 2.3540i$	$0.1167 \pm .0001 + (2.3543 \pm .0001)i$	

Table II. Values of the complex growth rate θ for different values of α and C.

RESISTIVE CASE

R	Theory	Simulation	α
0.05	-1.7642	-1.7633	$\pi/2$
0.2	-1.3587	-1.3564	
0.5	-0.8746	-0.8728	
2.0	-0.2908	-0.2905	
0.05	0.6407	0.6417	$3\pi/2$
0.2	0.4348	0.4353	
0.5	0.2674	0.2677	
2.0	0.09229	0.09235	
0.05	$0.1173 + 1.3827i$	$0.1170 \pm .0005 + (1.386 \pm .001)i$	$5\pi/2$
0.2	$-0.6762 + 0.9299i$	$-0.6810 \pm .0005 + (0.931 \pm .001)i$	
0.5	-0.33648	$-0.33640 \pm .00005$	
2.0	-0.06701	$-0.06778 \pm .00008$	

Table III. Values of the complex growth rate θ for different values of α and R.

Errors not shown are smaller than accuracy given.

INDUCTIVE CASE

L	Theory	Simulation	α
0.01	-0.0775 $+10.0537i$	-0.0777 $+10.0563i$	$\pi/2$
0.1	-0.56102 $+3.25597i$	-0.56109 $+3.25605i$	
1.0	-0.08775 $+0.81437i$	-0.08774 $+0.81438i$	
40.0	-0.0021749 $+0.12622i$	-0.0021747 $+0.12622i$	
0.01	0.74385	$0.744 \pm .001$	$3\pi/2$
0.1	0.61736	0.61748	
1.0	0.33751	0.33758	
40.0	0.06918	0.06919	
0.01	0.51971 $+1.2920i$	$0.520 \pm .001$ $+(1.2925 \pm .0005)i$	$5\pi/2$
0.1	0.25327 $+0.8424i$	0.25346 $+0.8427i$	
1.0	0.04338 $+0.3419i$	0.04342 $+0.3420i$	
40.0	0.001183 $+0.05635i$	$0.001184 \pm .000002$ $+0.05638i$	

Table IV. Values of the complex growth rate θ for different values of α and L.

Errors not shown are smaller than accuracy given.

LC MODE

L	Theory	Simulation
0.00112	-0.02978 $+29.92419i$	-0.02996 $+29.92480i$
0.0014	0.02521 $+26.77038i$	0.02536 $+26.77048i$
0.0018	-0.03906 $+23.62486i$	-0.03921 $+23.62513i$
0.0024	0.03147 $+20.47098i$	0.03159 $+20.47098i$
0.0034	-0.05696 $+17.21925i$	-0.05709 $+17.21943i$
0.0050	0.04128 $+14.22469i$	0.04136 $+14.22464i$
0.0085	-0.10147 $+10.95935i$	-0.10156 $+10.95951i$
0.0170	0.05809 $+7.83190i$	0.05815 $+7.83185i$

Table V. Complex growth rate for $\alpha = \pi/2$ and various small values of L.

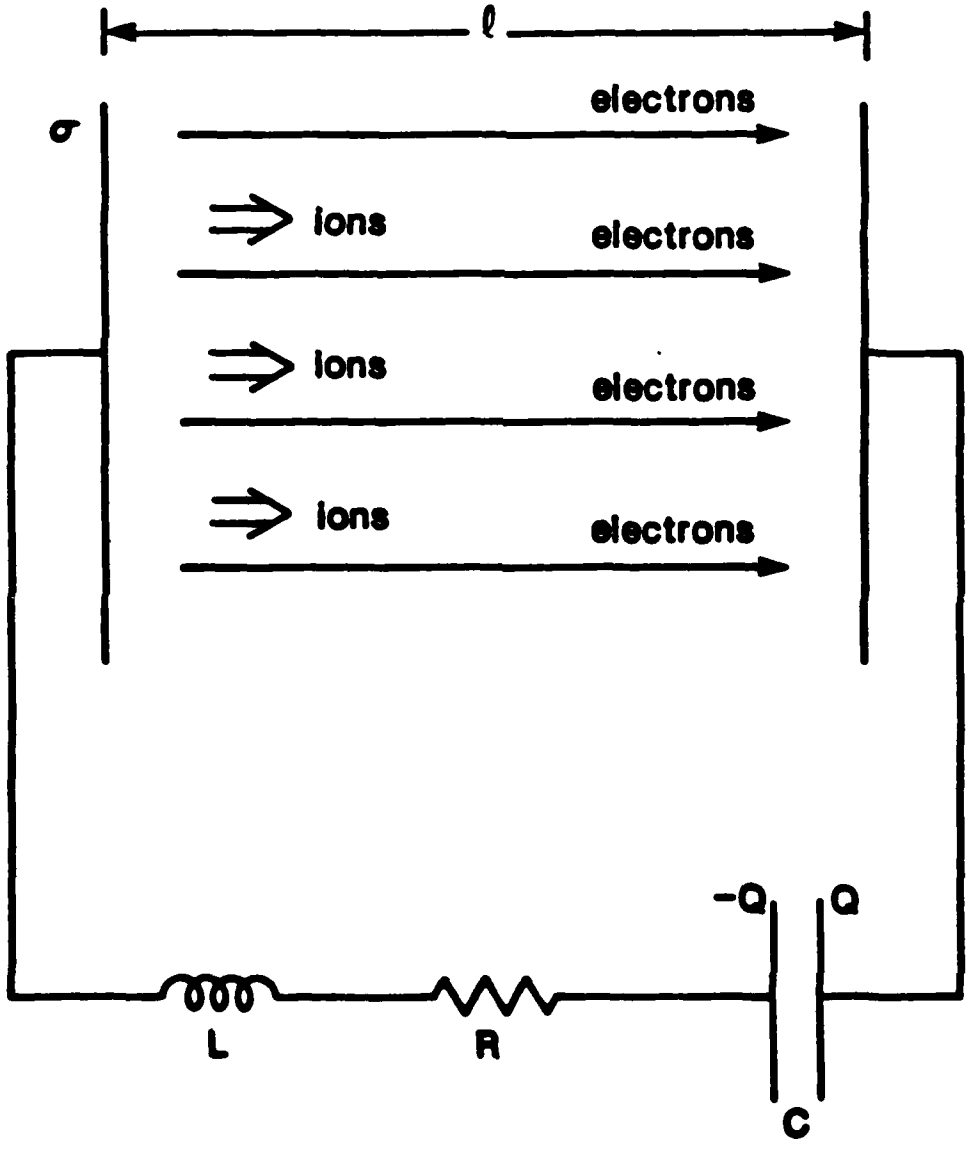

Fig. 1. Extended Pierce model. Note that the ground symbol denotes only the reference potential. No charge can flow to this ground since the model is one-dimensional.

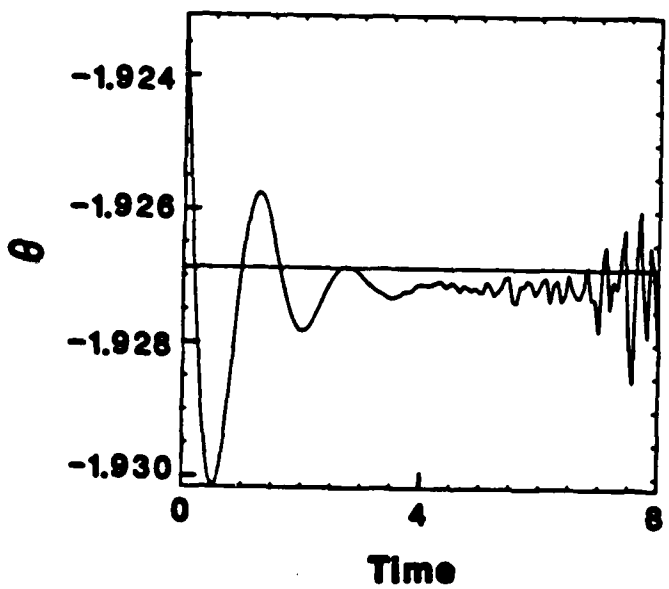

Fig. 2. Typical history of growth-rate diagnostic. Accuracy is limited first by competing modes, then by numerical noise. The analytic answer is $\theta = -1.9269$.)

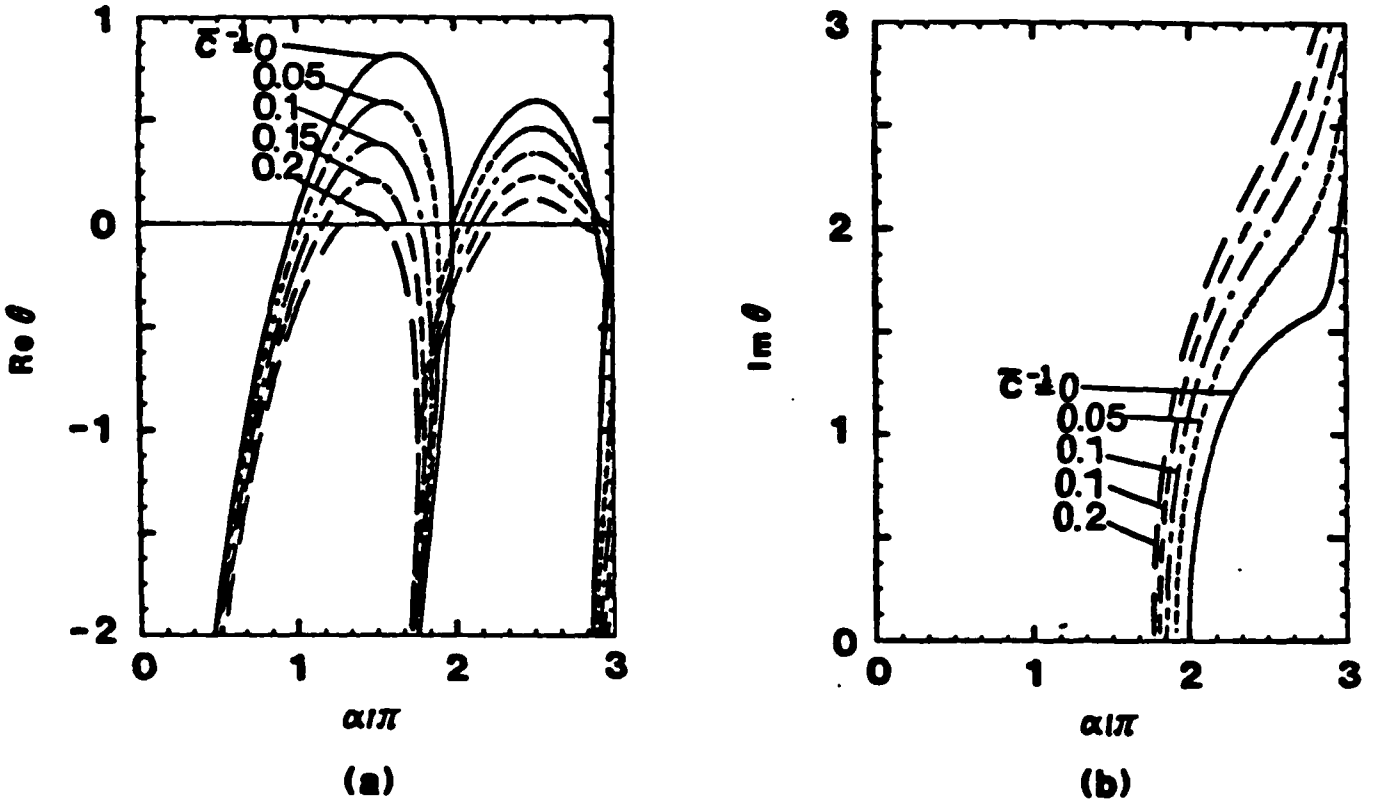

Fig. 3. Real and imaginary parts of the complex growth rate versus α for several values of C. (From Kuhn and Hörhager.)

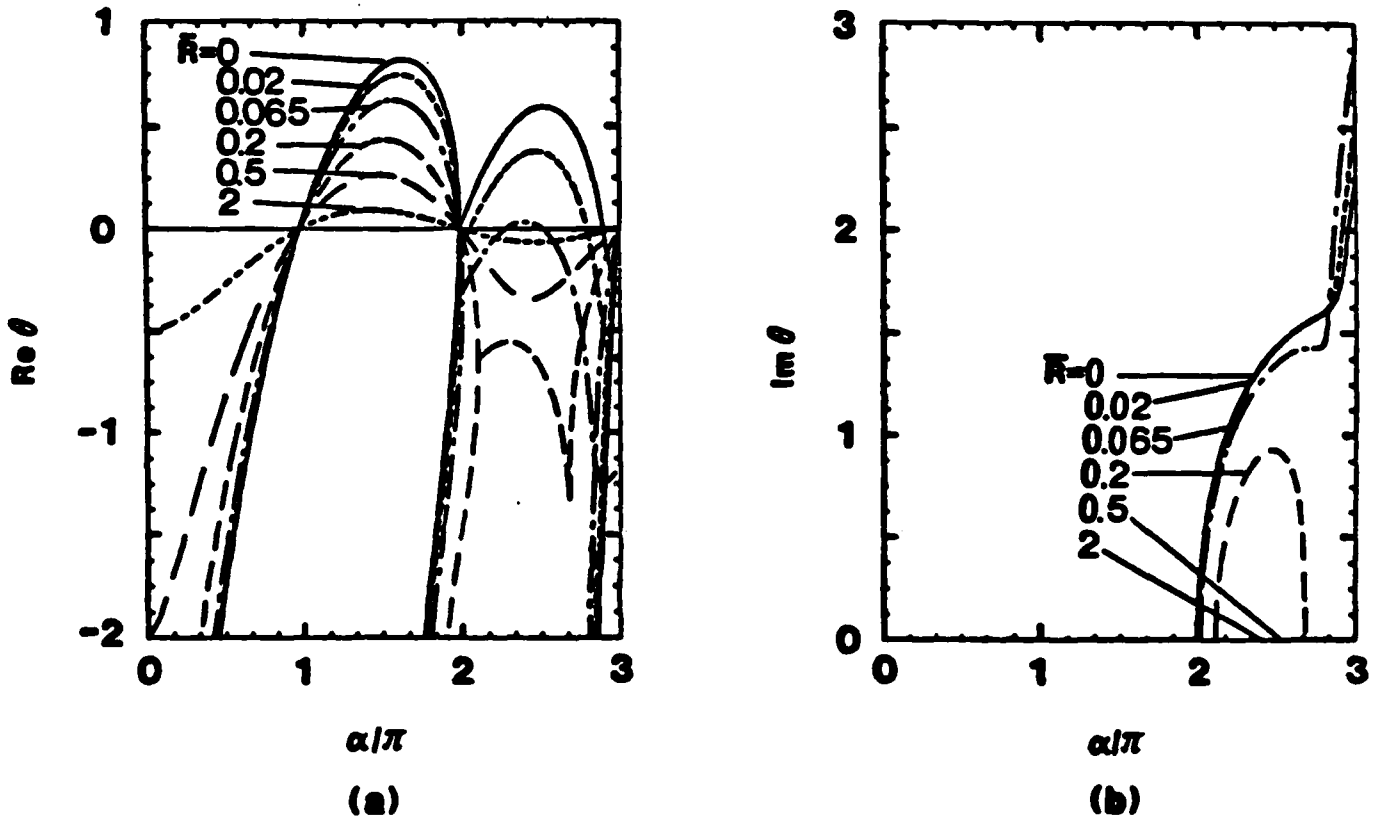

Fig. 4. Real and imaginary parts of the complex growth rate versus α for several values of R. (From Kuhn and Hörhager.)

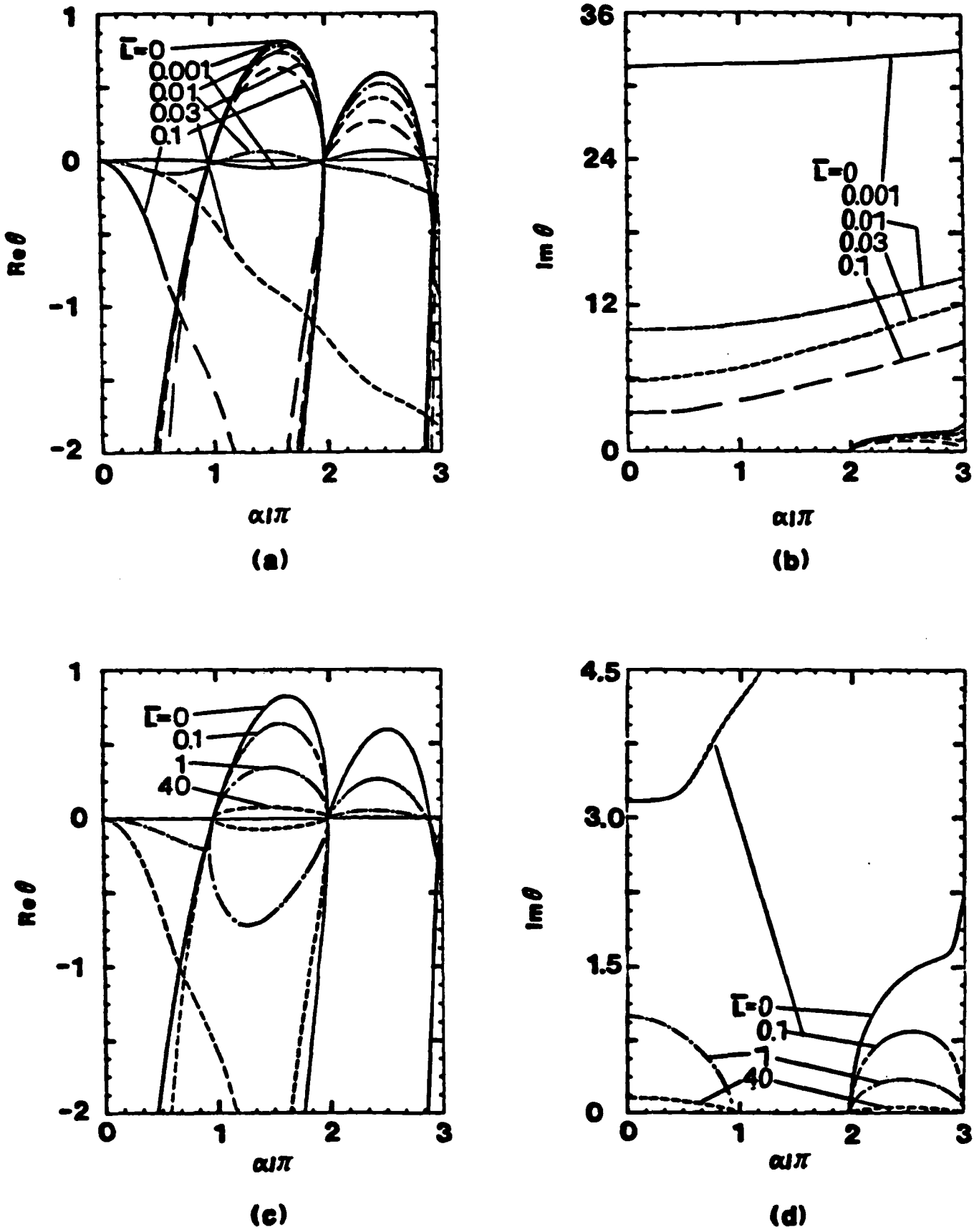

Fig. 5. Real and imaginary parts of the complex growth rate versus α over a wide range of values of L. (From Kuhn and Hörhager.)

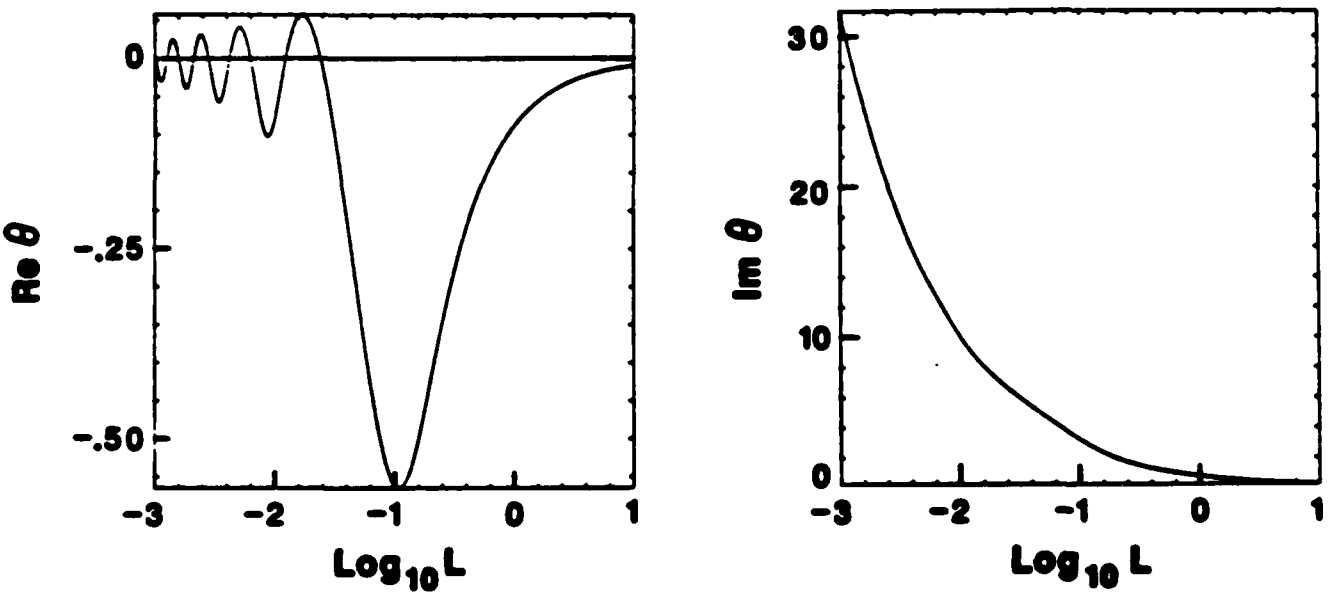

Fig. 6. Real and imaginary parts of the complex growth rate versus $\log_{10} L$ at $\alpha = \pi/2$. (From Kuhn and Hörhager.)

END

Feb.

1988

DTIC